

COGNITIVE NEUROSCIENCE

Neural correlate of spatial (mis-)localization during smooth eye movements

Stefan Dowiasch,¹ Gunnar Blohm² and Frank Bremmer¹¹Department of Neurophysics, Philipps-University Marburg, Karl-von-Frisch-Straße 8a, 35043 Marburg, Germany²Queen's University, Kingston, ON, Canada**Keywords:** eye-position decoding, macaque area VIP, mislocalization, smooth pursuit

Edited by John Foxe

Received 17 October 2015, accepted 19 April 2016

Abstract

The dependence of neuronal discharge on the position of the eyes in the orbit is a functional characteristic of many visual cortical areas of the macaque. It has been suggested that these eye-position signals provide relevant information for a coordinate transformation of visual signals into a non-eye-centered frame of reference. This transformation could be an integral part for achieving visual perceptual stability across eye movements. Previous studies demonstrated close to veridical eye-position decoding during stable fixation as well as characteristic erroneous decoding across saccadic eye-movements. Here we aimed to decode eye position during smooth pursuit. We recorded neural activity in macaque area VIP during steady fixation, saccades and smooth-pursuit and investigated the temporal and spatial accuracy of eye position as decoded from the neuronal discharges. Confirming previous results, the activity of the majority of neurons depended linearly on horizontal and vertical eye position. The application of a previously introduced computational approach (isofrequency decoding) allowed eye position decoding with considerable accuracy during steady fixation. We applied the same decoder on the activity of the same neurons during smooth-pursuit. On average, the decoded signal was leading the current eye position. A model combining this constant lead of the decoded eye position with a previously described attentional bias ahead of the pursuit target describes the asymmetric mislocalization pattern for briefly flashed stimuli during smooth pursuit eye movements as found in human behavioral studies.

Introduction

Eye-position signals ('Gain fields' or 'eye-position fields') are ubiquitous in the visual cortical system of the macaque. They have been found in striate (Trotter & Celebrini, 1999), extrastriate (Galletti & Battaglini, 1989; Bremmer *et al.*, 1997a; Bremmer, 2000), parietal (Andersen & Mountcastle, 1983; Bremmer *et al.*, 1997b, 1999; Morris *et al.*, 2012, 2013) and even in the premotor cortex (Boussaoud *et al.*, 1998). Gain fields are hypothesized to be of critical importance for a stable perception of our environment (Zipser & Andersen, 1988; Bremmer *et al.*, 1998; Snyder *et al.*, 1998; Boussaoud & Bremmer, 1999; Salinas & Abbott, 2001; Blohm *et al.*, 2009; Blohm, 2012).

Eye-position decoding typically has been applied to the stationary case, i.e., the fixating eye. It was only recently that decoding was introduced to the dynamic case (Morris *et al.*, 2012, 2013; Xu *et al.*, 2012). By investigating saccades Morris and colleagues (2013) showed that eye-position signals in four cortical areas of the macaque, among them the ventral intraparietal area (VIP), are precise on short time scales. Yet, eye-position decoding was not veridical in the temporal vicinity of saccades. Instead, the decoded eye position

was leading the real eye position briefly before the onset of a saccade, but lagging at the end (Morris *et al.*, 2012). This bi-phasic error pattern resembled results from human psychophysical studies on the localization of perisaccadic visual stimuli. The authors suggested that the erroneous eye-position signal could be the neural basis of the observed behavioral phenomenon.

Localization errors occur also during smooth eye movements: pursuit onset (Blanke *et al.*, 2010), steady-state pursuit (Mateeff *et al.*, 1981; van Beers *et al.*, 2001; Königs & Bremmer, 2010), anticipatory pursuit (Blohm *et al.*, 2003) and optokinetic nystagmus, OKN (Kaminiazar *et al.*, 2007). During OKN, stimulus locations across the whole visual field are perceptually shifted in the direction of its slow phase. During pursuit, however, spatial localization is asymmetric. Mislocalization occurs only in the hemifield ahead of the pursuit target. The neural bases of these perceptual phenomena are as yet unclear. Given the above described results on saccades, we hypothesized that continuous eye-position decoding across SPEM is possible but likely not veridical. We reanalyzed data from the macaque area VIP which had previously been recorded while monkeys performed SPEMs in otherwise darkness (Schlack *et al.*, 2003). By employing isofrequency decoding (Boussaoud & Bremmer, 1999), we found that decoded eye position was not veridical but leading the actual eye position. Smooth pursuit induces an attention-field centered

Correspondence: Frank Bremmer, as above.
E-mail: frank.bremmer@physik.uni-marburg.de

ahead of the pursuit target (Khan *et al.*, 2010). Physiologically, attention is known to act on neurons in area VIP (Maunsell & Cook, 2002) and to induce a shift of visual receptive fields toward its center (Ben Hamed *et al.*, 2002; Womelsdorf *et al.*, 2006), leading to a perceptual expansion of space away from its center (Wardak *et al.*, 2011). We show that a model, combining two independent signal sources, i.e., an erroneous eye-position signal and a spatial signal derived from a visual map distorted by attention, can explain localization error during smooth eye movements.

Materials and methods

The current study is an extended computational analysis of neural and behavioral data reported before (Schlack *et al.*, 2003). Accordingly, the procedures described here focus on the analytical treatment of the data and provide only the most relevant specifics of the behavioral and electrophysiological procedures. Full details of experimental methods are provided in our previous report (Schlack *et al.*, 2003).

Animal preparation

Experimental and surgical preparation followed standard procedures. In brief, two monkeys were prepared for recordings under general anesthesia and under sterile surgical conditions. Each animal was implanted with a device for holding the head. Based on structural MRI scans a recording chamber for microelectrode penetrations through the intact dura was placed in a frontal plane at an angle of 45° with respect to the vertical for recordings in area VIP. Additionally, scleral search coils were implanted to monitor eye position (Judge *et al.*, 1980). During the experiment, the animal sat in a primate chair with the head restrained, facing a translucent screen and performing oculomotor tasks for liquid reward. All procedures were in accordance with published guidelines on the use of animals in research (European Council Directive 86/609/EEC) and were approved by the regional ethics committee.

Behavioral paradigm

Oculomotor targets (red LEDs, diameter: 0.8°, luminance: 0.4 cd/m²) were back projected onto a translucent screen (size: 90° × 90°) 48 cm in front of the monkey. All experiments were performed in the dark (luminance < 0.01 cd/m²). To prevent dark adaptation, room lights were briefly switched on prior to a new set of trials for at least a couple of seconds.

In the saccade paradigm, a central fixation target was presented for 1000 ms, followed by a 10° step, pseudo-randomly chosen into one of four directions (left, right, up, and down). The animals' task was to perform a saccade to the target location within 500 ms and keep fixation until the end of the trial (2.5 s). Smooth pursuit eye movements were induced by a Rashbass-'step-ramp-paradigm' (Rashbass, 1961). Here, the target moved in pseudo-randomized order at 10°/s into one of four directions (left, right, up, and down). After initial presentation of a central fixation target (800 ms) the target was shifted by 10° in the direction opposite to the following smooth pursuit direction and started to move instantaneously for 1500 ms. Accordingly, each trial had a total duration of 2.3 s.

Binocular eye movements were continuously recorded at 200 Hz in the pursuit task and at 500 Hz in the saccade task. In the pursuit task, only trials without any catch-up saccades were analyzed further. Neurons were isolated and their corresponding spikes were detected on-line. Spike-times were stored for offline analysis with

1 ms resolution. For each neuron recorded, the saccade and pursuit paradigms were performed consecutively with the order counterbalanced across recordings without a specific adjustment of the experimental parameters to the specific functional properties of the neuron (e.g. receptive field location, size, etc.). We recorded at least 20 trials for each neuron and stimulus direction for each paradigm resulting in a minimum total number of 160 trials per neuron.

Data analysis

Eye-movement data and neuronal activity were analyzed with MATLAB 2012a (The MathWorks Inc., Natick, USA). Saccade onset was determined by a velocity criterion with a threshold of 80°/s in a time window of 0–400 ms after target displacement. Spike times were converted into a spike density function, which averaged across all trials for each condition, using a Gaussian smoothing with a standard deviation of the Gaussian kernel of $\sigma = 30$ ms and a Gaussian filter with a window size of $6 * \sigma - 1$ (Silverman, 1986). Noise correlations were not analyzed separately. Eye-position signals were smoothed with the same set of filters. Eye movement and neural data were aligned to saccade onset.

Isofrequency decoding

Extracellular neural activity as obtained during steady fixation in the saccade paradigm was used to determine an eye-position field for each of the 180 neurons recorded. Many previous studies have shown the eye-position effect to be linear along the horizontal and vertical eye position, also in area VIP (Bremmer *et al.*, 1999). Accordingly, we fitted two-dimensional linear regression functions to the neuronal discharges (Fig. 1). A regression plane represents the tuning of a cell for eye position: the gradient represents the direction of the steepest increase in activity with eye position, the intercept determines the average discharge of the neuron. Regression planes were fitted into the average neural discharges obtained long before (pre-saccadic: – 700 to – 200 ms) and long after saccade onset (post-saccadic: + 300 to + 900 ms). During these epochs, the eyes were constantly positioned either at the screen center (pre-saccadic. $[x, y] = [0^\circ, 0^\circ]$) or at one of the four eccentric fixation locations (post-saccadic. $[x, y] = [\pm 10^\circ, 0^\circ], [0^\circ, \pm 10^\circ]$). By choosing these analysis windows, we excluded interference of eye-position-dependent neuronal discharges with saccade planning and/or execution. This is supported by the analysis of the mean activity of the 180 neurons during saccades in each of the four directions. Figure 2 shows, that up to 200 ms before saccade onset and from 300 ms after saccade onset on, the firing rate of the population of neurons was not significantly different from baseline activity. This is in line with previous studies in area VIP which showed that excitability of VIP neurons is back to normal about 300 ms after saccade onset (Bremmer *et al.*, 2009). For each cell, the values of the regression plane as determined from the saccade paradigm were applied to neural activity recorded in the pursuit paradigm. This allowed us to decode eye position continuously across the SPEM by employing an isofrequency decoding regime, which has been employed as an analytical tool to extract eye-position signals from neuronal recordings in various brain regions before (Boussaoud & Bremmer, 1999). This population decoder is based on the planar tuning of the eye-position signals. For a given eye position, a neuron fires at a specific frequency. Yet, due to the planar tuning, this discharge occurs not only for one single eye position, but for a whole range of eye positions. In a mathematical sense, the discharge occurs for an infinite number of eye positions, all located along a straight line perpendicular to

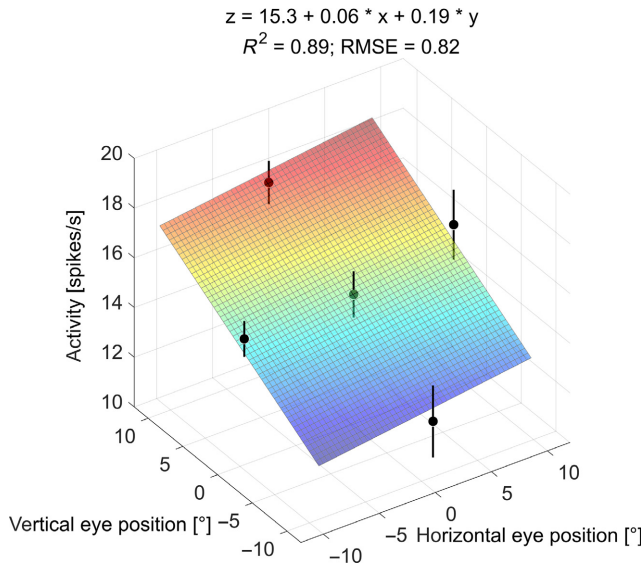


FIG. 1. Eye-position tuning of one representative example neuron during the saccade paradigm. The color-coded plane represents the two-dimensional linear regression of the neuronal activity as a function of five different eye positions averaged over a pre- and post-saccadic time epoch from -700 to -200 ms and 300 to 900 ms around saccade onset (black dots). The black vertical lines show the standard deviation of the mean at each data point. The regression equation and its goodness-of-fit parameters are given above the figure.

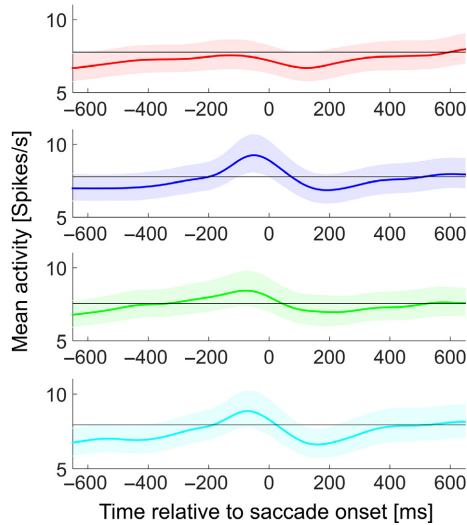


FIG. 2. Mean activity of the population of neurons as a function of time in the saccade paradigm. The color-coded lines show the mean activity of 180 neurons in area VIP of two macaque monkeys during the performance of saccades to the right (red), left (blue), up (green) and down (cyan) and their corresponding 95% confidence intervals. The baseline activity (solid black line) was computed as the median of the activity from each neuron in the interval 200 ms before and 300 ms after saccade onset. There was no significant deviation from baseline activity long before and after the execution of the saccade.

the gradient of the regression plane, the so-called ‘isofrequency line’. Accordingly, discharges from a single neuron are not sufficient to decode eye position unequivocally. Considering discharges from a second neuron, however, theoretically would be sufficient, given that the second neuron would have a different tuning for eye position. In such case, also for this second neuron an isofrequency line on its regression plane could be found. This line, however, would

be differently oriented in the 2-D eye-position space. The only point located simultaneously on both isofrequency lines is the point of intersection (PI) of these lines, which represents the current eye position.

This scenario reflects the ideal case of a perfect linear fit of a 2-D regression plane to the neuronal discharges and constant discharges over time. Due to temporal fluctuations of the neural signal and due to imperfect 2-D linear fits, the PI obtained from two single neurons is typically only a coarse measure of the current eye position. Hence, the isofrequency regime considers the PIs obtained from a whole population of neurons, constructed from a sequence of serial recordings: for n neurons, these are $(n * (n + 1)/2)$ PIs. The decoded eye position is computed as the median of the distribution of all PIs.

Attention and localization during smooth pursuit

Localization of briefly flashed stimuli during smooth pursuit induces an attentional field which is broadly ahead of the pursuit target (Khan *et al.*, 2010). Attention induces (or is based on) a shift of visual receptive fields toward the attended location (Ben Hamed *et al.*, 2002; Womelsdorf *et al.*, 2006). This shift of visual RFs in turn leads to a perceptual expansion of visual space (Wardak *et al.*, 2011). We modeled such an expansion based on the structure of the attentional field during smooth pursuit as given by Khan *et al.* (2010), i.e., their equation for saccade reaction times during smooth pursuit, given in the legend of their Fig. 8. These authors found that attention is broadly ahead of the pursuit target and that this attentional field could be fitted by a 2-D sigmoid with a superimposed Gaussian:

$$L_{\text{attention}} = -0.010 + 0.065 / (1 + \exp(0.328 * (x - 4.24))) + 0.05 * \exp(-((x - 4.734)^2 + (y - 0.081)^2) / 5.8032) \quad (1)$$

Boundary conditions of our model of perceptual expansion of space due to attention resulted from behavioral data in humans showing (i) almost no mislocalization during SPEM in the visual hemifield behind the pursuit target and (ii) smaller localization error in the directions perpendicular to the pursuit direction (van Beers *et al.*, 2001; Königs & Bremmer, 2010). In our model, overall localization error then results from superimposing two signals: (i) decoded eye position and (ii) a visual map, distorted by attention.

Statistical analysis

To statistically evaluate the mean relative error of the decoded eye-position signal over time we calculated a moving average using a bootstrap analysis with 50 000 iterations (Efron, 1979). As the real and the decoded eye position were sampled with 200 Hz, we randomly took samples with replacement from the relative error of the decoded eye-position signal in the four different stimulus directions (left, right, up, and down) within a time-window of ± 25 ms around each 5 ms time step. We chose this short time window in order to have a sufficient number of spikes available for the bootstrapping to provide robust results. This analysis provided 95% confidence intervals, which were used to assess significance levels.

Results

This study is based on recordings from 180 neurons in area VIP of two macaque monkeys. The discharges related to smooth pursuit eye-movements have been described in detail before (Schlack *et al.*,

2003). Here, we focused on the decoding of eye-position signals from these neuronal discharges. In addition to smooth pursuit eye movements, monkeys performed in separate sets of trials visually guided saccades. Discharges during continuous, steady fixation long before or long after a saccade were used to determine a neuron's eye-position field. An example for such an eye-position-dependent modulation of spontaneous activity during active fixation is shown in Fig. 1. For this neuron, the strongest activity was observed for fixation up and to the right (reddish colors), while lowest discharges were observed for fixation left and down. The 2-D regression plane could be fitted significantly to the cell's discharges. This result confirms data from previous studies (Bremmer *et al.*, 1999; Morris *et al.*, 2012). During steady fixation, a given eye position results in a certain neuronal discharge. This discharge, however, does not occur only for a single eye position. Instead, it occurs, in a mathematical sense, for an infinite number of eye positions, all located along a straight line. For the example neuron in Fig. 1, such lines are represented by identical color values on the 2-D regression plane. As shown previously (Boussaoud & Bremmer, 1999), real eye position should be given by the median of the pairwise points of intersection (PIs) of a population of cells. Indeed, based on the discharges of the whole population of VIP neurons, decoded eye positions during steady fixation were close to the real eye positions (Fig. 3, gray areas). During steady fixation prior to the saccade, i.e., in a time window from $t = 400$ to 200 ms before saccade onset, the mean error was $\varepsilon = 0.001^\circ$, which was not significantly different from zero (95% confidence interval = $[-0.62^\circ, 0.69^\circ]$, bootstrapped with 50 000 iterations; Fig. 3). An analog result was obtained for steady fixation well after the saccade, i.e., from $t = 300$ to 500 ms after the onset of the saccade. Here, the mean error $\varepsilon = -0.06^\circ$ again was not significantly different from zero (95% confidence interval = $[-0.66^\circ, 0.49^\circ]$, bootstrapped with 50 000 iterations; Fig. 3).

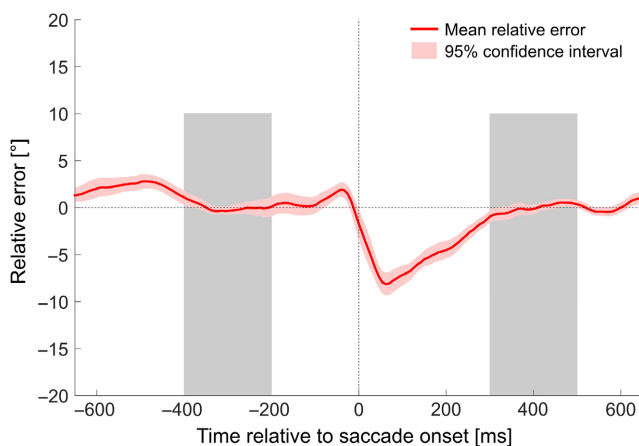


FIG. 3. Mean relative error of the decoded eye position as a function of time in the saccade paradigm. Time-resolved mean relative error of the decoded eye position with a bootstrapped 95% confidence interval based on recordings from 180 neurons in area VIP of two macaque monkeys. Bootstrap statistics were obtained by randomly selecting 50 000 samples with replacement from the relative error of all four saccade directions within a time window of ± 25 ms around each point in time. The mean relative error and the corresponding 95% confidence interval around zero degree during steady fixation prior, i.e., from $t = -400$ to -200 ms (left gray area) and after, i.e., from $t = 300$ to 500 ms (right gray area) the saccade indicates an accurate representation of eye position during steady fixation. The mean relative error increased after initiation of the saccade in direction opposite to it, represented by a negative relative error.

Continuous decoding of eye position

In a second step, we analyzed the accuracy of the decoded eye position outside steady fixation, i.e., across the saccades. Confirming previous results (Morris *et al.*, 2012, 2013), our analysis revealed a bi-phasic perisaccadic error pattern (Fig. 3). A subtle increase in error in the direction of the upcoming saccade was followed by a large error in the direction opposite to the saccade.

In a third step of our analysis, we aimed to decode eye position during smooth pursuit. Eye movements had been recorded in a classical Rashbass paradigm (Rashbass, 1961). After initial fixation, the target stepped in pseudo-randomized order into one of four directions (right, up, left, or down) and instantaneously started to move in the opposite direction. Critically, for decoding, we applied the regression plane values as obtained from the saccade paradigm to the neuronal discharges recorded during smooth pursuit. In other words: the neural samples, from which the fit parameters were obtained, were different from the samples, to which the decoding algorithm was applied.

Well before pursuit onset, i.e., in a temporal window from $t = 400$ to 200 ms before onset of the initial catch-up saccade, the mean relative error of the decoded eye position was minimal ($\varepsilon = -0.06^\circ$) and not significantly different from zero (95% confidence interval = $[-1.78^\circ, 1.72^\circ]$, bootstrapped with 50 000 iterations). After a minimal negative blip, it increased markedly in direction of the upcoming pursuit around the time of the catch-up saccade (Fig. 4A). As the initial saccade was in the opposite direction to the pursuit, this effect equals the pattern observed in the saccade paradigm. After the catch-up saccade and its related decoding error, the relative error decreased to an almost constant level. Around 300 ms after the onset of the catch-up saccade, the gain of the smooth pursuit eye movement reached an almost constant value for the duration of the eye movement with a mean of 0.97 (95% confidence interval = $[0.95, 0.98]$, bootstrapped with 50 000 iterations; Fig. 4B). During this steady-state pursuit, i.e., in the time window from $t = 300$ to 1000 ms after saccade onset, the mean decoding error was 1.38° . A positive value indicates a lead of the decoded eye position in the direction of the pursuit as compared to the actual eye position. This lead of decoded eye position was statistically significant (95% confidence interval = $[0.21^\circ, 2.68^\circ]$, bootstrapped with 50 000 iterations; Fig. 4A). Even when shifting the time window marking the steady-state pursuit by the mean duration of the catch-up saccades (60 ms), the lead of the decoded eye position was statistically significant with a mean of 1.26° (95% confidence interval = $[0.09^\circ, 2.54^\circ]$, bootstrapped with 50 000 iterations).

Furthermore, we analyzed the influence of the distance between the actual eye position and the pursuit target during steady-state pursuit and performed a multiple regression analysis with this parameter and the steady state pursuit gain as well as the relative error of the decoded eye position (Fig. 4C). On average, the actual eye position was 0.13° behind the pursuit target. If the actual eye position lagged behind the pursuit target, the gain was generally higher and the relative error of the decoded eye position was small. If the actual eye position was leading the pursuit target, the gain was smaller and the relative error of the decoded eye position was larger. A stepwise examination of this multiple regression showed that using all three parameters generated the best fit of the data ($R^2 = 0.46$; RMSE = 3.09; $P = 4.65 \times 10^{-74}$) as compared to a single linear regression of distance and relative decoding error ($R^2 = 0.43$; RMSE = 3.16; $P = 1.82 \times 10^{-70}$), the sole linear regression of distance and Gain ($R^2 = 0.28$; RMSE = 0.043; $P = 1.11 \times 10^{-41}$), or

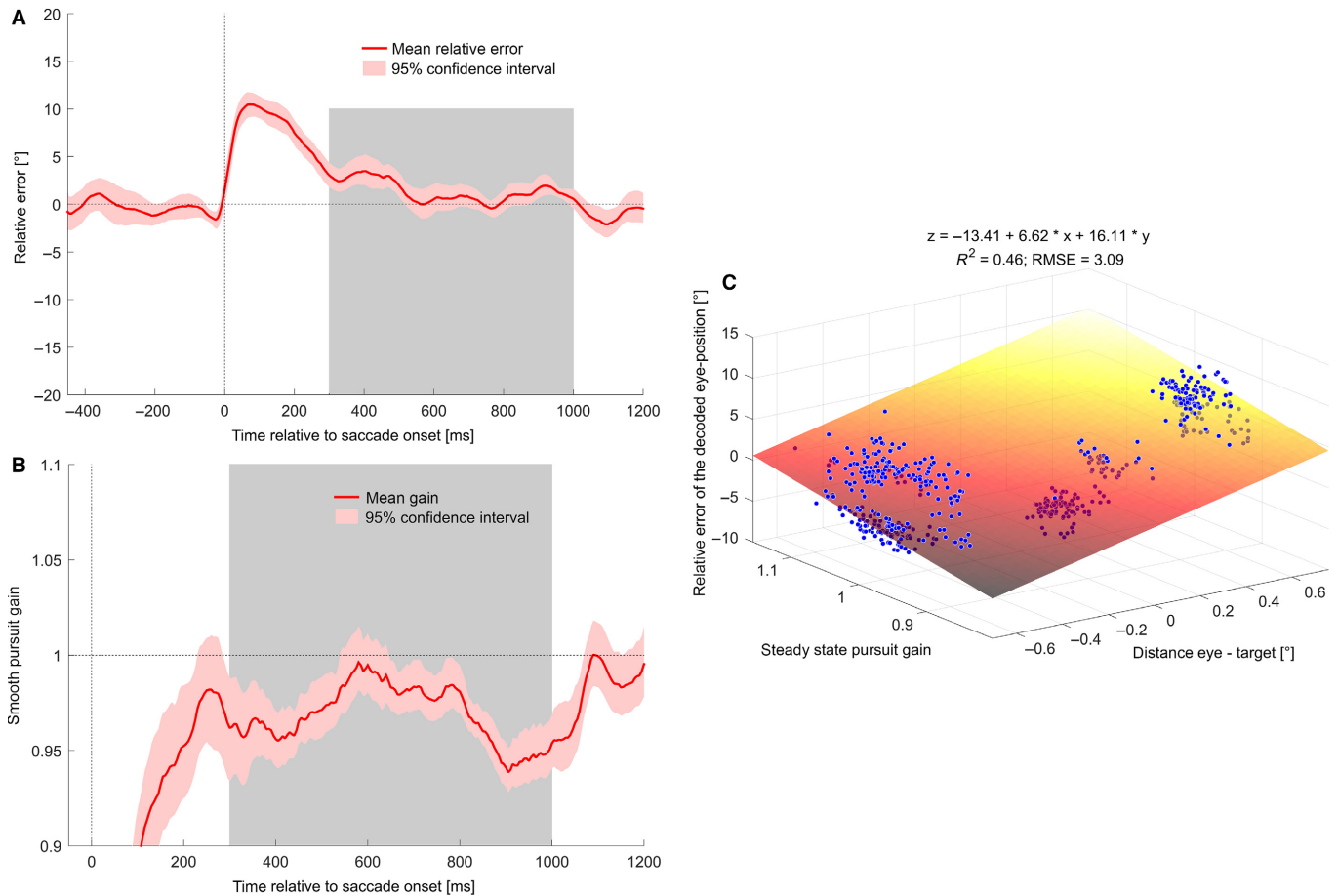


FIG. 4. Mean relative error of the decoded eye position and smooth pursuit gain as a function of time in the pursuit paradigm. (A) Time-resolved mean relative error of the decoded eye position with a bootstrapped 95% confidence interval based on recordings from 180 neurons in area VIP of two macaque monkeys. Bootstrap statistics were obtained by randomly selecting 50 000 samples with replacement from the relative error of all four pursuit directions within a time-window of ± 25 ms around each point in time. As for the saccade paradigm, the relative error of the decoded eye position was largest around the time of the saccade due to a shift of the decoded eye position in the direction opposite to the saccade, i.e., the direction of the upcoming pursuit. During steady-state pursuit, i.e., from $t = 300$ to 1000 ms (right gray area), the decoded eye position showed a lead ahead of the actual eye position indicated by the positive mean relative error of 1.38° on average. Bootstrapped 95% confidence interval averaged across the entire time period of steady state pursuit (gray area) was significantly bigger than zero [0.21° , 2.68°]. (B) Smooth pursuit gain as a function of time. Around 300 ms after the initial catch-up saccade, the smooth pursuit gain reached an almost constant level in the time window of steady-state pursuit (gray area) with a mean of 0.97 and little variation. Bootstrap statistics for the 95% confidence interval was obtained by randomly selecting 50 000 samples with replacement from the gain of all four pursuit directions within a timewindow of ± 25 ms around each point in time. Bootstrapped 95% confidence interval averaged across the entire time period of steady-state pursuit was [0.95; 0.98]. (C) The color-coded plane represents the linear regression of the distance between the actual eye position and pursuit target (x -axis), the steady-state pursuit gain (y -axis) and the relative decoding error (z -axis). A positive distance between the eye and the pursuit target indicates a lead of the eye. Likewise, a positive relative error of the decoded eye position indicates a lead of the decoded eye-position signal as compared to the actual eye position. The figure shows that if the actual eye position lagged behind the pursuit target, the gain was generally higher and the relative error of the decoded eye position was smaller. If the actual eye position was ahead of the pursuit target, the gain was smaller and the relative error of the decoded eye position was larger.

relative decoding error and Gain ($R^2 = 0.043$; $RMSE = 4.1024$; $P = 8.13 \times 10^{-7}$).

Finally, we investigated the influence of smooth pursuit velocity on the relative error of the decoded eye position. To this end, we computed the relative decoding error in a subset of 78 neurons for three different pursuit velocities ($5^\circ/s$, $10^\circ/s$ and $20^\circ/s$). These neurons were only tested during pursuit in the preferred direction of each neuron (Fig. 5). The mean relative error during steady-state pursuit was positive for all three pursuit velocities and could be explained by a constant temporal lead of the internal eye-position signal of about 200 ms. To estimate the maximum achievable accuracy of a whole population of neurons in area VIP, we computed the mean error of the decoded eye position as a function of the number of cells contributing to the isofrequency coding (Fig. 6).

This was done by randomly selecting 100 000 subsets of neurons from the 180 measured neurons. This procedure was repeated for each of the given population sizes. Figure 6 shows that the absolute error of the decoded eye position decreases with an increasing number of cells approximately following an inverse square-root function. Using this correlation, we can calculate the theoretically needed number of neurons to achieve a defined accuracy, e.g. about 900 neurons are needed for a continuous representation of eye position during SPEM with a mean absolute error $< 2^\circ$.

Decoded eye position and attention

Given that a functional equivalent of macaque area VIP has been identified in the human parietal cortex (Bremmer *et al.*, 2001;

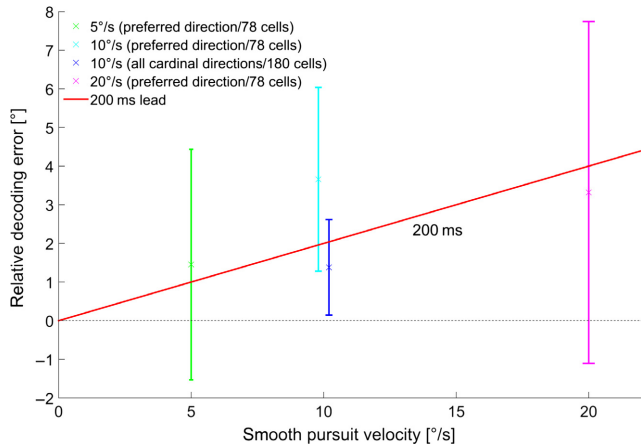


FIG. 5. Mean relative error of the predicted eye position as a function of pursuit velocity. Mean relative errors (marked by a cross) decoded from all available neurons and error bars representing the standard deviations over the time of the steady state pursuit, i.e., from $t = 300$ to 1000 ms after the initial saccade. For all measured pursuit velocities, the internal eye-position signal as leading the actual eye position, i.e., $1.45^\circ \pm 2.98^\circ$ for a pursuit velocity of $5^\circ/\text{s}$, $3.66^\circ \pm 2.39^\circ$ for $10^\circ/\text{s}$ and $3.32^\circ \pm 4.42^\circ$ for $20^\circ/\text{s}$. The relation between the relative error of the decoded eye position and the pursuit velocity could be described best by a constant temporal lead of the internal representation of eye position by about 200 ms.

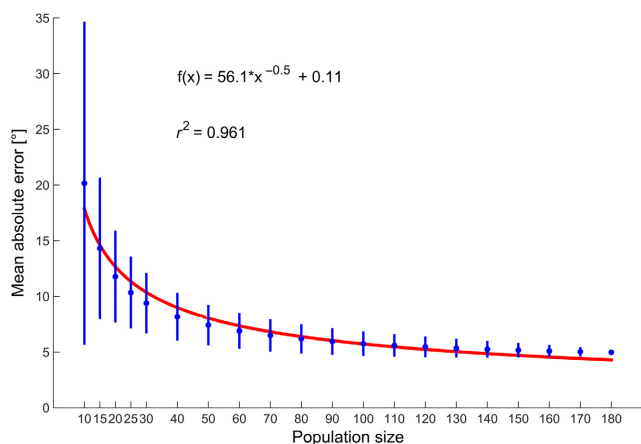


FIG. 6. Mean absolute error of the predicted eye position as compared to the real eye position during smooth pursuit as a function of population size of neurons in area VIP. Mean errors (blue dots) and standard deviations (blue lines) were computed by randomly selecting $100\,000$ subsets of neurons from each given sample size ($n = 10, 15, 20, 25, 30, 40, \dots$). This led to a monotonically decreasing error with an increasing number of neurons, which could be fitted by an inverse square root function. This functional approach suggests a highly accurate and reliable representation of eye-position information in the whole population of neurons in area VIP, e.g. roughly 900 neurons are needed for an internal eye-position representation during SPEM with a mean deviation of $< 2^\circ$.

Sereno & Huang, 2006, 2014), erroneous eye-position signals most likely also exist in the human visual cortical system. Accordingly, if spatial localization would rely among other signals on an estimate of eye position, a constant lead of decoded eye position would suggest a shift of perceived spatial locations in the direction of pursuit across the whole visual field. Such a constant perceptual shift has been described for the slow phases of optokinetic look nystagmus (Kaminiazar *et al.*, 2007). During pursuit, however, mislocalization is only found in the visual hemifield ahead of the fovea. In order to

explain this asymmetry in spatial localization during SPEM, we suggest an additional mechanism to act in concert with the erroneous eye-position signal: attention. Attention has been shown to lead to a perceptual distortion of space, i.e., an expansion of perceived locations away from the focus of attention (Wardak *et al.*, 2011). Khan and colleagues (2010) have mapped the attentional field during the presentation of briefly flashed targets during pursuit, which could be fitted by a 2-D sigmoid with a superimposed Gaussian, and found attention centered broadly ahead of pursuit, resulting in an asymmetry with respect to the fovea. We hence modeled the effect of attention on spatial localization by transforming the attentional map as given by Khan *et al.* (2010) into a (mis-)localization map:

$$L_{\text{attention}} = -\mathbf{65} * (-\mathbf{0.0848} + 0.065 / (1 + \exp(0.328 * (x - 4.24)))) + 0.05 * \exp(-((x - 4.734)^2 + (y - 0.081)^2) / 5.8032) \quad (2)$$

In this Eqn 1, only the scaling factors (highlighted in bold) were changed as compared to the findings of Khan *et al.* (2010). These factors were adjusted to meet the boundary condition of localization, i.e., only a marginal error in the hemifield behind the fovea. According to our hypothesis, localization during smooth pursuit should be given by a superposition of the erroneous eye-position signal and the spatial map, which is distorted by attention:

$$L = L_{\text{eye.pos.}} + L_{\text{attention}} \quad (3)$$

The resulting 2-D error pattern for localizing stimuli during smooth pursuit is shown in Fig. 7. Horizontal localization error starts to build up at the vertical meridian. Vertical localization error is directed away from the focus of attention. This error pattern qualitatively resembles the behavioral data observed in humans (van Beers *et al.*, 2001; Königs & Bremmer, 2010).

Discussion

Efference copy vs. proprioception

Over the last three decades, numerous studies have shown that neurons in many visual cortical areas of the macaque carry an eye-position signal (e.g. Andersen & Mountcastle, 1983; Galletti & Battaglini, 1989; Bremmer *et al.*, 1997a,b; Trotter & Celebrini, 1999; Bremmer, 2000), among them also area VIP (Duhamel *et al.*, 1997; Bremmer *et al.*, 1999; Morris *et al.*, 2012, 2013). A number of different approaches have shown that the functional characteristics of these modulatory influences of eye position on neuronal discharge are suited to decode eye position from the activity of a population of neurons within each of these areas: a back-propagation network (Andersen & Mountcastle, 1983), splitting a population into two sub-populations with opposite tuning properties (Bremmer *et al.*, 1998), an isofrequency decoding (Boussaoud & Bremmer, 1999), as well as a maximum likelihood approach (Morris *et al.*, 2012, 2013).

Eye-position signals have also been documented for neurons in the primary somatosensory cortex (Wang *et al.*, 2007; Xu *et al.*, 2011). Based on this finding, it was suggested that eye-position signals result from proprioception rather than from an efference copy or from corollary discharge. In line with this hypothesis, it was shown that the strength of visual responses of a number of neurons from area LIP visually stimulated briefly after the end of a saccade was more compatible with pre-saccadic rather than post-saccadic eye positions (Xu *et al.*, 2012). These findings are in contrast to

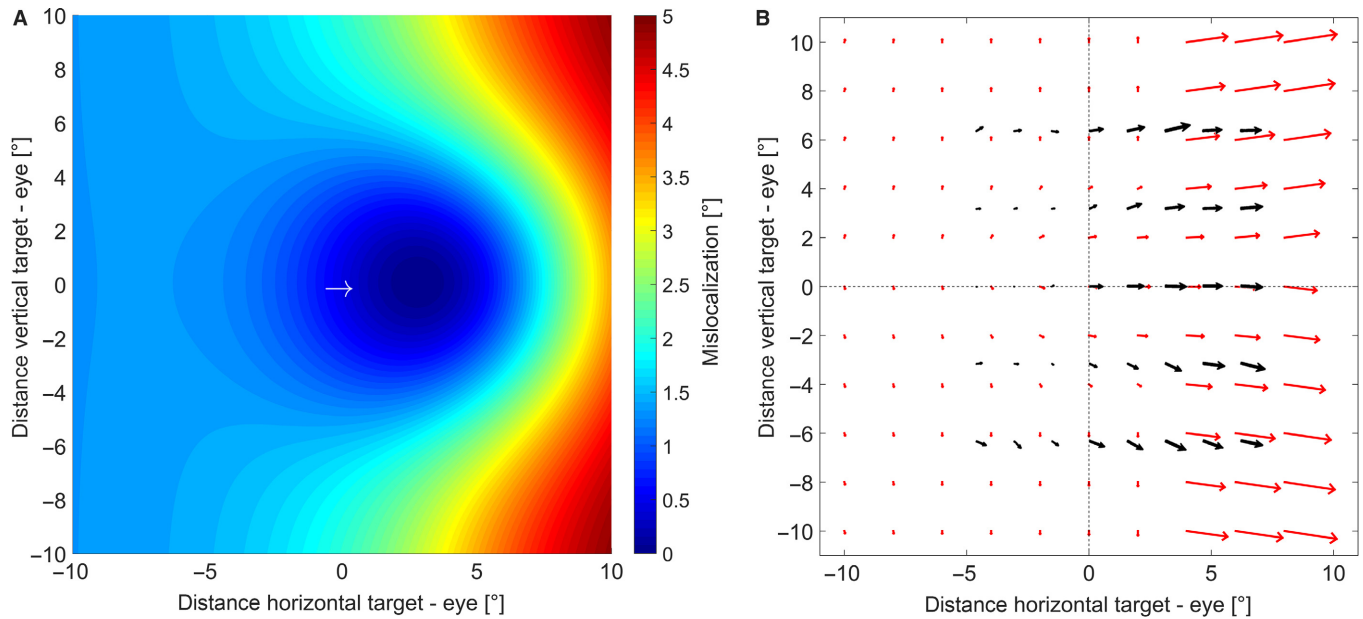


FIG. 7. Modeled mislocalization during SPEM. (A) The attention map found by Khan *et al.* (2010) was transferred to represent spatial perception during smooth pursuit. As shown before, focused attention induces perceptual shifts away from the focus. In order to meet boundary conditions, the first two constant scaling factors of the 2-D sigmoid and superimposed Gaussian fit function found by Khan *et al.* (2010) were adjusted: $z = -65 * (-0.0848 + 0.065 / (1 + \exp(0.328 * (x - 4.24)))) + 0.05 * \exp(-((x - 4.734)^2 + (y - 0.081)^2) / 5.8032)$. The arrow illustrates the direction of pursuit with the head marking the location of the pursuit target. (B) Shown as red arrows is the cumulative mislocalization from the combination of attentional effects and a constant lead of the decoded eye-position signal of about 1.4° as found in our study. Both sources of mislocalization add up in the visual hemifield ahead of the pursuit target and almost neutralize each other in the hemifield behind the eye. The resulting model (red arrows) closely resembles the behaviorally measured asymmetric mislocalization pattern typically observed during smooth pursuit eye movements (black arrows, van Beers *et al.*, 2001).

results from two other recent studies (Morris *et al.*, 2012, 2013). Here, Morris and colleagues tested the time course of the pure eye-position signals without any further visual stimulation in four different cortical areas of the macaque dorsal visual pathway: areas MT, MST, LIP, and VIP. The authors unequivocally showed that eye position as decoded from population activity within each of these areas started to change prior to saccade onset. Such a predictive change cannot be based on proprioception but rather would be indicative of an efference copy or corollary discharge signal. Our findings on decoded eye position leading the actual eye position during smooth pursuit are in agreement with the results from Morris and colleagues on saccades.

Continuous decoding of eye position

The result on the accuracy of decoded eye position during steady fixation in our study was in line with those of previous studies on dorsal visual areas (Boussaoud & Bremmer, 1999; Morris *et al.*, 2013). To decode the eye position during smooth pursuit eye movements, we used the 2-D linear tuning of each cell as computed from the saccade paradigm and applied it to the neuronal discharges as recorded during SPEM. The error of the decoded eye position during the initial fixation and the saccade to the pursuit target was in the same range and direction as in the saccade paradigm.

In line with previous studies, our data show that eye-position signals in area VIP are accurate and sufficiently fast to serve as a possible candidate for representing the actual eye position not only during steady fixation, but also during ongoing eye movements. The analysis of absolute decoding error as a function of population size showed, that there is a relationship between these parameters proportional to the inverse square root, which has been shown suitable for population coding of other parietal areas (Bremmer *et al.*, 1998;

Morris *et al.*, 2013) as well as premotor areas (Boussaoud & Bremmer, 1999) and primary visual cortex (Vogels, 1990). This functional approach suggests a highly accurate and reliable efference copy signal during SPEM available from the whole population of VIP neurons. Hence, they provide viable information for a coordinate transformation of visual signals from an eye-centered to a head-centered frame of reference at the population level. Such a transformation is thought to be necessary not only for a stable perception of our environment (Zipser & Andersen, 1988; Salinas & Abbott, 2001; Bremmer, 2005), but also for the computation of pursuit motor commands in the correct reference frame (Blohm & Lefèvre, 2010; Murdison *et al.*, 2015). It remains to be determined, if explicit head-centered representations at the single cell level, which have been shown for area VIP during steady fixation (Duhamel *et al.*, 1997; Avillac *et al.*, 2005; Schlack *et al.*, 2005), can also be found across eye movements.

During steady-state pursuit, the relative error of the decoded eye position was positive. Such a positive error indicates that the internal representation of eye position was slightly leading the actual eye position. However, it is unlikely that this lead is due to an underestimating of eye eccentricity, which has been found in extrastriate cortex (Morris *et al.*, 2013). Such an underestimation would produce a lead of the decoded eye position when the pursuit target moves toward the center of the screen and would turn into a lag when the target moves away from the center. Yet, as shown in Fig. 4A, the lead of the decoded eye position remained almost constant for the entire duration of steady-state pursuit, even after crossing the center of the screen at around 800 ms after saccade onset, due to the mean latency of 200 ms of the initial catch-up saccade.

The multiple regression analysis of the three parameters 'distance between actual eye position and pursuit target', 'pursuit gain' and 'relative decoding error' revealed further insight into how the

decoded eye position might be influenced by other eye movement parameters. First of all, the smooth pursuit eye movement in our study showed a typical feature of ringing (Robinson *et al.*, 1986), i.e., a lead of the actual eye position relative to the pursuit target induced a gain below one, whereas a lag of the actual eye position lead to a gain higher than one. Yet, the mean pursuit gain of 0.97 averaged across all trials was well within the usual range of a typical smooth pursuit task (e.g. Lisberger *et al.*, 1981; Lencer *et al.*, 2004; Konen *et al.*, 2005). Furthermore, the comparison of the distance between the actual eye position and the pursuit target with the relative decoding error showed that the decoded eye position was leading the pursuit target on average by 1.27°. Yet, our results show, that pursuit velocity influences the relative decoding error. Although the data is quite noisy because of the smaller number of neurons in the velocity dependent measurement and because there is no one-to-one mapping between the 10°/s measurement in all cardinal directions vs. the preferred direction, the relationship between relative decoding error and pursuit velocity can be translated into a constant temporal lead of the internal representation of eye position of about 200 ms. This phenomenon, historically called 'perception time' (Hazelhoff & Wiersma, 1924; Mita *et al.*, 1950), has been described by previous psychophysical studies and was reported to be within the same range (Brenner *et al.*, 2001; Rotman *et al.*, 2002, 2005; Kerzel *et al.*, 2006). In addition, this timing fits nicely with the time which the saccadic system needs to account for future changes of the pursuit target and perform a catch-up saccade (de Brouwer *et al.*, 2001, 2002; Orban de Xivry & Lefèvre, 2007). Thus, it seems that eye position coding in VIP predicts the location of the target about 200 ms into the future, which might be used for the programming of catch-up saccades during the steady-state pursuit.

On the other hand, the finding of a lead of the decoded eye position in relation to the actual eye position could explain, at least in part, the behaviorally observed mislocalization of briefly flashed stimuli during SPEM (Mateeff *et al.*, 1981; van Beers *et al.*, 2001; Königs & Bremmer, 2010) or related smooth eye movements like the slow phase of optokinetic nystagmus (Kaminiarz *et al.*, 2007): if the erroneously decoded eye position would be combined with information about the location of a visual stimulus on the retina, it could induce the above mentioned mislocalization. Similarly, a possible neural substrate of the mislocalization during saccades had been identified (Morris *et al.*, 2012).

Indeed, the mean relative error of about 1.4° for the whole population of 180 neurons measured with a velocity of 10°/s in our current study greatly matches the mean localization error reported during the slow phase of look nystagmus (Kaminiarz *et al.*, 2007; Tozzi *et al.*, 2007). In these experiments, visual stimuli were presented during ongoing OKN. When stimulus presentation fell in a slow phase of the OKN, stimuli were mislocalized in the direction of the eye movements. Stimuli, which were presented shortly before, during or after a fast phase of the OKN were mislocalized according to a saccade-like error pattern. These results were very different from results during stare-nystagmus or during Optokinetic Afternystagmus (OKAN), which can be induced by prolonged optokinetic stimulation. In such a case, mislocalization during the slow phase was not in the direction of the eye movements, but directed away from the fovea, resulting in a perceptual expansion of space (Kaminiarz *et al.*, 2008). Interestingly, only SPEM and look nystagmus are associated with very similar cortical activation patterns in motion sensitive and eye-movement areas (Konen *et al.*, 2005), which is not the case for stare-nystagmus and OKAN. These results suggest that visual localization during eye movements,

which are under cortical control, relies (at least in part) on decoded eye-position signals.

Decoded eye position and attention

If localization was based only on an erroneous eye-position signal, perceived positions of briefly flashed stimuli should always be shifted in the direction of the eye movement, irrespective of the position of this stimulus in the visual field. Yet, different from look nystagmus, mislocalization during smooth pursuit is asymmetric with respect to an eye-centered visual field: it is found almost exclusively in the visual hemifield ahead of the pursuit target (or the fovea) (van Beers *et al.*, 2001; Königs & Bremmer, 2010). There it increases from about 2° for stimuli close to the fovea to a maximum value of up to 5° for stimuli presented further away from the fovea. This suggests an additional signal contributing to the mislocalization during SPEM in addition to the erroneously decoded eye position.

Visual receptive fields have been shown to shift toward the location where attention is allocated (Ben Hamed *et al.*, 2001; Womelsdorf *et al.*, 2006). If the spotlight of attention coincides with the fovea, the receptive fields shift toward the fovea. According to a labeled line coding, this centripetal shift must result in a centrifugal shift of perceptual localization with respect to the fovea. Such a centrifugal shift away from the focus of attention has recently been demonstrated in behavioral experiments in humans (Wardak *et al.*, 2011). During smooth pursuit, however, attention is not always where the fovea is. Instead, a study of Khan *et al.* (2010) found that attention during SPEM is allocated broadly ahead of the pursuit target. By mapping response latencies to visual stimuli presented around the pursuit target, a peak of attention was found at about 4° ahead of the pursuit target. By considering different eye velocities, the authors found that there was a constant lead of attention in time, not in space, i.e., the faster the eye velocity, the further ahead was attention. Accordingly, this spatial attention most likely induces an asymmetric distortion of perceptual space with perceived locations directed away from the center (or focus) of attention. Figure 7A shows the function of the attentional field during SPEM found by Khan *et al.* (2010) converted to represent (mis-)localization under the assumption that the location with the highest attention shows the least mislocalization. This attentional landscape can be considered a potential field implying a centrifugal force always directed away from its center. Importantly, this spatially asymmetric signal alone would not be sufficient to explain mislocalization during pursuit: in such case, stimulus positions in the hemifield the eye comes from should be mislocalized in the direction opposite to the pursuit direction. Hence, we suggest that this distorted representation of perceptual space is superimposed onto the erroneously decoded eye-position signal. The combination of a spatial map, distorted by attention, and a constant lead of the decoded eye position would add up to a joint localization map.

In this map, the effects of attention and decoded eye position add to each other in the visual hemifield ahead of the focus of attention, but antagonize each other in the hemifield behind the fovea (Fig. 7B). The resulting error map qualitatively resembles the asymmetric localization error during smooth pursuit as found in behavioral experiments in humans (van Beers *et al.*, 2001; Königs & Bremmer, 2010). The mislocalization studies during smooth pursuit eye movements to which we refer all used flashed targets as localization stimuli. We thus only used established results from the attention literature that are compatible with this paradigm, i.e., Blohm *et al.* (2005), Kanai *et al.* (2003), Tanaka *et al.* (1998), Van Donkelaar & Drew (2002) and Khan *et al.* (2010). Other paradigms such

as a target discrimination task (Khurana & Kowler, 1987; Souto & Kerzel, 2008; Lovejoy *et al.*, 2009) might lead to different attentional allocations and therefore different localization patterns for which our model might not be suitable. Further discussion of this topic can be found in Khan *et al.* (2010).

As OKN is a reflexive eye movement, it is assumed that attention is uniformly allocated across the whole visual field. Without a specific attentional contribution only the constant lead of the decoded eye position would induce a uniform mislocalization pattern across the visual field. Indeed, such an error pattern has been shown for the slow phase of look-OKN (Kaminiazar *et al.*, 2007). Accordingly, our data suggest that it should be possible to decode eye position from neural activity in the macaque area VIP (and most likely further visual cortical areas with eye-position-dependent activation) during the slow phases of look nystagmus. Most likely, this decoded signal would not be veridical but rather show a lead with respect to real eye position.

To the best of our knowledge, this is the first study to show the predictive nature of eye-position signals during smooth pursuit eye movements at a neuronal level. Simultaneously, we used this finding to provide a potential physiological explanation for the behaviorally observed localization errors of flashed targets during smooth eye movements. Whether such a mechanism is actually used by the brain to determine a spatial representation across smooth eye movements and what brain areas contribute the most, however, cannot be answered by currently available data sets.

Conflict of interest

The authors declare no conflict of interests.

Acknowledgements

This work was supported by the 'Deutsche Forschungsgemeinschaft' (DFG) International Research Training Group IRTG 1901 'The Brain in Action – BrainAct', the Collaborative Research Center CRC/TRR-135/A1 and FOR 1847-A2.

Abbreviations

LIP, lateral intraparietal (area); MRI, magnetic resonance imaging; MST, medial superior temporal (area); MT, middle temporal (area); OKAN, optokinetic afternystagmus; OKN, optokinetic nystagmus; PI, point of intersection; RF, receptive field; RMSE, root mean square error; SPEM, smooth pursuit eye movement; VIP, ventral intraparietal (area).

References

Andersen, R.A. & Mountcastle, V.B. (1983) The influence of the angle of gaze upon the excitability of the light-sensitive neurons of the posterior parietal cortex. *J. Neurosci.*, **3**, 532–548.

Avillac, M., Deneve, S., Olivier, E., Pouget, A. & Duhamel, J.-R. (2005) Reference frames for representing visual and tactile locations in parietal cortex. *Nat. Neurosci.*, **8**, 941–949.

van Beers, R.J., Wolpert, D.M. & Haggard, P. (2001) Sensorimotor integration compensates for visual localization errors during smooth pursuit eye movements. *J. Neurophysiol.*, **85**, 1914–1922.

Ben Hamed, S., Duhamel, J.-R., Bremmer, F. & Graf, W. (2001) Representation of the visual field in the lateral intraparietal area of macaque monkeys: a quantitative receptive field analysis. *Exp. Brain Res.*, **140**, 127–144.

Ben Hamed, S., Duhamel, J.-R., Bremmer, F. & Graf, W. (2002) Visual receptive field modulation in the lateral intraparietal area during attentive fixation and free gaze. *Cereb. Cortex*, **12**, 234–245.

Blanke, M., Harsch, L., Knöll, J. & Bremmer, F. (2010) Spatial perception during pursuit initiation. *Vision. Res.*, **50**, 2714–2720.

Blohm, G. (2012) Simulating the cortical 3D visuomotor transformation of reach depth. *PLoS One*, **7**, e41241.

Blohm, G. & Lefèvre, P. (2010) Visuomotor velocity transformations for smooth pursuit eye movements. *J. Neurophysiol.*, **104**, 2103–2115.

Blohm, G., Missal, M. & Lefèvre, P. (2003) Smooth anticipatory eye movements alter the memorized position of flashed targets. *J. Vision*, **3**, 10.

Blohm, G., Missal, M. & Lefèvre, P. (2005) Processing of retinal and extraretinal signals for memory-guided saccades during smooth pursuit. *J. Neurophysiol.*, **93**, 1510–1522.

Blohm, G., Keith, G.P. & Crawford, J.D. (2009) Decoding the cortical transformations for visually guided reaching in 3D space. *Cereb. Cortex*, **19**, 1372–1393.

Boussaoud, D. & Bremmer, F. (1999) Gaze effects in the cerebral cortex: reference frames for space coding and action. *Exp. Brain Res.*, **128**, 170–180.

Boussaoud, D., Joffrais, C. & Bremmer, F. (1998) Eye position effects on the neuronal activity of dorsal premotor cortex in the macaque monkey. *J. Neurophysiol.*, **80**, 1132–1150.

Bremmer, F. (2000) Eye position effects in macaque area V4. *NeuroReport*, **11**, 1277–1283.

Bremmer, F. (2005) Navigation in space – the role of the macaque ventral intraparietal area. *J. Physiol.*, **566**, 29–35.

Bremmer, F., Distler, C. & Hoffmann, K.P. (1997a) Eye position effects in monkey cortex. II. Pursuit-and fixation-related activity in posterior parietal areas LIP and 7A. *J. Neurophysiol.*, **77**, 962.

Bremmer, F., Ilg, U.J., Thiele, A., Distler, C. & Hoffmann, K.P. (1997b) Eye position effects in monkey cortex. I. Visual and pursuit-related activity in extrastriate areas MT and MST. *J. Neurophysiol.*, **77**, 944.

Bremmer, F., Pouget, A. & Hoffmann, K.-P. (1998) Eye position encoding in the macaque posterior parietal cortex. *Eur. J. Neurosci.*, **10**, 153–160.

Bremmer, F., Graf, W., Ben Hamed, S. & Duhamel, J.-R. (1999) Eye position encoding in the macaque ventral intraparietal area (VIP). *NeuroReport*, **10**, 873–878.

Bremmer, F., Schlack, A., Shah, N.J., Zafiris, O., Kubischik, M., Hoffmann, K.-P., Zilles, K. & Fink, G.R. (2001) Polymodal motion processing in posterior parietal and premotor cortex: a human fMRI study strongly implies equivalencies between humans and monkeys. *Neuron*, **29**, 287–296.

Bremmer, F., Kubischik, M., Hoffmann, K.-P. & Krekelberg, B. (2009) Neural dynamics of saccadic suppression. *J. Neurosci.*, **29**, 12374–12383.

Brenner, E., Smeets, J.B.J. & van den Berg, A.V. (2001) Smooth eye movements and spatial localisation. *Vision. Res.*, **41**, 2253–2259.

de Brouwer, S., Missal, M. & Lefèvre, P. (2001) Role of retinal slip in the prediction of target motion during smooth and saccadic pursuit. *J. Neurophysiol.*, **86**, 550–558.

de Brouwer, S., Missal, M., Barnes, G. & Lefèvre, P. (2002) Quantitative analysis of catch-up saccades during sustained pursuit. *J. Neurophysiol.*, **87**, 1772–1780.

Duhamel, J.-R., Bremmer, F., BenHamed, S. & Graf, W. (1997) Spatial invariance of visual receptive fields in parietal cortex neurons. *Nature*, **389**, 845–848.

Efron, B. (1979) Bootstrap methods: another look at the jackknife. *Ann. Stat.*, **7**, 1–26.

Galletti, C. & Battaglini, P.P. (1989) Gaze-dependent visual neurons in area V3A of monkey prestriate cortex. *J. Neurosci.*, **9**, 1112–1125.

Hazelhoff, F.F. & Wiersma, H. (1924) Die Wahrnehmungszeit. *Z. Psychol.*, **96**, 171–188.

Judge, S.J., Richmond, B.J. & Chu, F.C. (1980) Implantation of magnetic search coils for measurement of eye position: an improved method. *Vision. Res.*, **20**, 535–538.

Kaminiazar, A., Krekelberg, B. & Bremmer, F. (2007) Localization of visual targets during optokinetic eye movements. *Vision. Res.*, **47**, 869–878.

Kaminiazar, A., Krekelberg, B. & Bremmer, F. (2008) Expansion of visual space during optokinetic afternystagmus (OKAN). *J. Neurophysiol.*, **99**, 2470–2478.

Kanai, R., van der Geest, J. & Frens, M. (2003) Inhibition of saccade initiation by preceding smooth pursuit. *Exp. Brain Res.*, **148**, 300–307.

Kerzel, D., Aivar, M.P., Ziegler, N.E. & Brenner, E. (2006) Mislocalization of flashes during smooth pursuit hardly depends on the lighting conditions. *Vision. Res.*, **46**, 1145–1154.

Khan, A.Z., Lefèvre, P., Heinen, S.J. & Blohm, G. (2010) The default allocation of attention is broadly ahead of smooth pursuit. *J. Vision*, **10**, 7.

Khurana, B. & Kowler, E. (1987) Shared attentional control of smooth eye movement and perception. *Vision. Res.*, **27**, 1603–1618.

- Konen, C.S., Kleiser, R., Seitz, R.J. & Bremmer, F. (2005) An fMRI study of optokinetic nystagmus and smooth-pursuit eye movements in humans. *Exp. Brain Res.*, **165**, 203–216.
- Königs, K. & Bremmer, F. (2010) Localization of visual and auditory stimuli during smooth pursuit eye movements. *J. Vision*, **10**, 8.
- Lencer, R., Nagel, M., Sprenger, A., Zapf, S., Erdmann, C., Heide, W. & Binkofski, F. (2004) Cortical mechanisms of smooth pursuit eye movements with target blanking. An fMRI study. *Eur. J. Neurosci.*, **19**, 1430–1436.
- Lisberger, S.G., Evinger, C., Johanson, G.W. & Fuchs, A.F. (1981) Relationship between eye acceleration and retinal image velocity during foveal smooth pursuit in man and monkey. *J. Neurophysiol.*, **46**, 229–249.
- Lovejoy, L.P., Fowler, G.A. & Krauzlis, R.J. (2009) Spatial allocation of attention during smooth pursuit eye movements. *Vision Res.*, **49**, 1275–1285.
- Mateeff, S., Yakimoff, N. & Dimitrov, G. (1981) Localization of brief visual stimuli during pursuit eye movements. *Acta Psychol.*, **48**, 133–140.
- Maunsell, J.H.R. & Cook, E.P. (2002) The role of attention in visual processing. *Philos. T. Roy. Soc. B*, **357**, 1063–1072.
- Mita, T., Hironaka, K. & Koike, I. (1950) The influence of retinal adaptation and location on the “empfindungszeit”. *Tohoku J. Exp. Med.*, **52**, 397–405.
- Morris, A.P., Kubischik, M., Hoffmann, K.-P., Krekelberg, B. & Bremmer, F. (2012) Dynamics of eye-position signals in the dorsal visual system. *Curr. Biol.*, **22**, 173–179.
- Morris, A.P., Bremmer, F. & Krekelberg, B. (2013) Eye-position signals in the dorsal visual system are accurate and precise on short timescales. *J. Neurosci.*, **33**, 12395–12406.
- Murdison, T.S., Leclercq, G., Lefèvre, P. & Blohm, G. (2015) Computations underlying the visuomotor transformation for smooth pursuit eye movements. *J. Neurophysiol.*, **113**, 1377–1399.
- Orban de Xivry, J.-J. & Lefèvre, P. (2007) Saccades and pursuit: two outcomes of a single sensorimotor process. *J. Physiol.*, **584**, 11–23.
- Rashbass, C. (1961) The relationship between saccadic and smooth tracking eye movements. *J. Physiol.*, **159**, 326–338.
- Robinson, D.A., Gordon, J.L. & Gordon, S.E. (1986) A model of the smooth pursuit eye movement system. *Biol. Cybern.*, **55**, 43–57.
- Rotman, G., Brenner, E. & Smeets, J.B. (2002) Spatial but not temporal cueing influences the mislocalisation of a target flashed during smooth pursuit. *Perception*, **31**, 1195–1203.
- Rotman, G., Brenner, E. & Smeets, J.B.J. (2005) Flashes are localised as if they were moving with the eyes. *Vision Res.*, **45**, 355–364.
- Salinas, E. & Abbott, L.F. (2001) Chapter 11 Coordinate transformations in the visual system: how to generate gain fields and what to compute with them. In Nicolelis, M.A.L. (Ed.), *Progress in Brain Research, Advances in Neural Population Coding*. Elsevier, Amsterdam, pp. 175–190.
- Schlack, A., Hoffmann, K.-P. & Bremmer, F. (2003) Selectivity of macaque ventral intraparietal area (area VIP) for smooth pursuit eye movements. *J. Physiol.*, **551**, 551–561.
- Schlack, A., Sterbing-D’Angelo, S.J., Hartung, K., Hoffmann, K.-P. & Bremmer, F. (2005) Multisensory space representations in the macaque ventral intraparietal area. *J. Neurosci.*, **25**, 4616–4625.
- Sereno, M.I. & Huang, R.-S. (2006) A human parietal face area contains aligned head-centered visual and tactile maps. *Nat. Neurosci.*, **9**, 1337–1343.
- Sereno, M.I. & Huang, R.-S. (2014) Multisensory maps in parietal cortex. *Curr. Opin. Neurobiol.*, Neural maps, **24**, 39–46.
- Silverman, B.W. (1986) *Density Estimation for Statistical and Data Analysis*. Chapman and Hall, London.
- Snyder, L.H., Grieve, K.L., Brotchie, P. & Andersen, R.A. (1998) Separate body- and world-referenced representations of visual space in parietal cortex. *Nature*, **394**, 887–891.
- Souto, D. & Kerzel, D. (2008) Dynamics of attention during the initiation of smooth pursuit eye movements. *J. Vision*, **8**, 3.
- Tanaka, M., Yoshida, T. & Fukushima, K. (1998) Latency of saccades during smooth-pursuit eye movement in man. Directional asymmetries. *Exp. Brain Res.*, **121**, 92–98.
- Tozzi, A., Morrone, M.C. & Burr, D.C. (2007) The effect of optokinetic nystagmus on the perceived position of briefly flashed targets. *Vision Res.*, **47**, 861–868.
- Trotter, Y. & Celebrini, S. (1999) Gaze direction controls response gain in primary visual-cortex neurons. *Nature*, **398**, 239–242.
- Van Donkelaar, P. & Drew, A.S. (2002) The allocation of attention during smooth pursuit eye movements. In Hyona, J., Heide, D.P.M.W. & Radach, R. (Eds), *Progress in Brain Research, The Brain’s Eye: Neurobiological and Clinical Aspects of Oculomotor Research*. Elsevier, Amsterdam, pp. 267–277.
- Vogels, D.R. (1990) Population coding of stimulus orientation by striate cortical cells. *Biol. Cybern.*, **64**, 25–31.
- Wang, X., Zhang, M., Cohen, I.S. & Goldberg, M.E. (2007) The proprioceptive representation of eye position in monkey primary somatosensory cortex. *Nat. Neurosci.*, **10**, 640–646.
- Wardak, C., Denève, S. & Ben Hamed, S. (2011) Focused visual attention distorts distance perception away from the attentional locus. *Neuropsychologia*, **49**, 535–545.
- Womelsdorf, T., Anton-Erxleben, K., Pieper, F. & Treue, S. (2006) Dynamic shifts of visual receptive fields in cortical area MT by spatial attention. *Nat. Neurosci.*, **9**, 1156–1160.
- Xu, Y., Wang, X., Peck, C. & Goldberg, M.E. (2011) The time course of the tonic oculomotor proprioceptive signal in area 3a of somatosensory cortex. *J. Neurophysiol.*, **106**, 71–77.
- Xu, B.Y., Karachi, C. & Goldberg, M.E. (2012) The postsaccadic unreliability of gain fields renders it unlikely that the motor system can use them to calculate target position in space. *Neuron*, **76**, 1201–1209.
- Zipser, D. & Andersen, R.A. (1988) A back-propagation programmed network that simulates response properties of a subset of posterior parietal neurons. *Nature*, **331**, 679–684.